J Solid State Electrochem (2008) 12:757–763
DOI 10.1007/s10008-007-0429-7

ORIGINAL PAPER

The electrochemical polymerization of *o*-phenylenediamine on L-tyrosine functionalized glassy carbon electrode and its application

Lei Zhang · Jiying Lian

Received: 29 May 2007 / Revised: 2 September 2007 / Accepted: 2 September 2007 / Published online: 18 September 2007

Abstract The polymerization of *o*-phenylenediamine (OPD) on L-tyrosine (Tyr) functionalized glassy carbon electrode (GCE) and its electro-catalytic oxidation towards ascorbic acid (AA) had been studied in this report. L-Tyrosine was first covalently grafted on GCE surface via electrochemical oxidation, which was followed by the electrochemical polymerization of OPD on the L-tyrosine functionalized GCE. Then, the poly(*o*-phenylenediamine)/L-tyrosine composite film modified GCE (POPD-Tyr/GCE) was obtained. X-ray photo-electron spectroscopy (XPS), field emission scanning electron microscope (SEM), and electrochemical techniques have been used to characterize the grafting of L-tyrosine and the polymerization and morphology of OPD film on GCE surface. Due to the doping of the carboxylic functionalities in L-tyrosine molecules, the POPD film showed good redox activity in neutral medium, and thus, the POPD-Tyr/GCE exhibited excellent electrocatalytic response to AA in 0.1 mol l^{-1} phosphate buffer solution (PBS, pH 6.8). The anode peak potential of AA shifted from 0.58 V at GCE to 0.35 V at POPD-Tyr/GCE with a greatly enhanced current response. A linear calibration graph was obtained over the AA concentration range of 2.5×10^{-4}–1.5×10^{-3} mol l^{-1} with a correlation coefficient of 0.9998. The detection limit (3δ) for AA was 9.2×10^{-5} mol l^{-1}. The modified electrode showed good stability and reproducibility and had been used for the determination of AA content in vitamin C tablet with satisfactory results.

Keywords Poly(*o*-phenylenediamine)/L-tyrosine composite film · Ascorbic acid · *o*-phenylenediamine · L-Tyrosine

L. Zhang (✉) · J. Lian
Department of Chemistry, College of Life and Environment Science, Shanghai Normal University,
Shanghai 200234, People's Republic of China
e-mail: chemzl@shnu.edu.cn

Introduction

A considerable effort has been devoted to the development of voltammetric methods for the determination of ascorbic acid (AA) in biological samples for many years because ascorbic acid is a vital component in the diet of human, and it is known to take part in several biological reactions and is present in mammalian brain [1]. Recent clinical studies have demonstrated that the content of ascorbic acid in biological fluids can be used to assess the amount of oxidation stress in human metabolism [2], and excessive oxidative stress has been linked to cancer, diabetes mellitus, and hepatic disease. However, it is difficult to determine AA by direct oxidation at bare electrode because of the high over-potential, the fouling effect by its oxidation products, poor reproducibility, low selectivity, and poor sensitivity. Thus, much interest has been focused on the use of mediators and modified electrodes to catalyze the electrochemical oxidation of ascorbic acid. For example, various electrode surfaces modified with immobilized quinone groups [3], adsorbed TCNQ [4], deposited nickel pentacyanonitrosylferrate [5], covalently attached amino acids [6, 7], in-site functionalized self-assembled monolayer of 4-aminothiophenol [8], electro-polymerized films of polypyrrole [9, 10], and self-doped polyaniline (PAN) [11–13] have all been employed via mediator oxidation for the electrochemical investigation of AA.

Among the conducting polymers, PAN has attracted significant interest due to its high conductivity, good stability, and potential applications. Poly(*o*-phenylenediamine) (POPD), one of the most important derivatives of polyaniline, is also attractive because of its better performances of electroactivity, permselectivity, electrochromism and a wide application in electrocatalysis [14, 15], sensors [16–18], and electrochromics [19, 20]. However, the

electrochemical activity of POPD is also limited by medium pH just as that of PAN, and thus POPD shows nearly no electrochemical activity in neutral pH, which restricts its application in practice, especially in bioelectrochemistry. Thus, it is significant to develop new methods to extend the redox activity of POPD in a wide pH range.

In our study, L-tyrosine was first covalently grafted on glassy carbon electrode (GCE) surface by amino cation radicals to form the L-tyrosine functionalized GCE (Tyr/GCE) via electrochemical oxidation; then, the polymerization of OPD was carried out on Tyr/GCE. Thus, poly (*o*-phenylenediamine)/L-tyrosine composite film modified GCE (POPD-Tyr/GCE) was fabricated. In this study, it was found that the POPD doped by carboxylic functionalities exhibited improved electrochemical activity even up to neutral medium, and thus POPD-Tyr/GCE can be used for the electrocatalytic oxidation of AA in pH 6.8 phosphate buffer solution (PBS).

Experimental

Chemicals and solutions

OPD was obtained from Sigma and used after twice recrystallization from water. L-Tyrosine and acetonitrile (ACN) were purchased from Sinopharm Chemical Reagent and used as received. AA (Fluka Chemicals) solution was prepared with 0.1 mol l^{-1} PBS (pH 6.8) immediately before use. Sulfuric acid solutions (pH 1–3), 0.1 mol l^{-1} acetate (pH 4–5), 0.1 mol l^{-1} PBS (pH 6–8), and 0.1 mol l^{-1} borate (pH 9) buffers were used. Other reagents were all of analytical grade and used as received, and twice distilled water was used for the preparation of all the above solutions.

All experiments were carried out at room temperature (≈20 °C).

Apparatus

Cyclic voltammetry measurements were carried out using a CHI 660B electrochemical workstation (CH Instruments, USA) with a home-made three-electrode electrochemical cell, GCE (∅=3 mm) and POPD-Tyr/GCE were used as working electrodes, a platinum sheet (1×0.5 cm) as auxiliary electrode, and a saturated calomel electrode (SCE) as reference electrode.

X-ray photo-electron spectroscopy (XPS) was recorded on an ESCALAB-MKII spectrometer (VG, UK) with a Mo Kα X-rays radiation as the X-ray source for excitation. The data were obtained at room temperature, and typically, the operating pressure in the analysis chamber was below 10^{-9} Torr with an analyzer pass energy of 50 eV. The resolution was 0.2 eV.

A JXA 840 field emission scanning electron microscope (SEM, JEOL, Japan) was used to examine the morphology of the polymer film.

Preparation of the modified electrode

GCE was first polished carefully with alumina powder (1.0, 0.5 and 0.03 μm, successively) on a wet soft polishing cloth. After being sonicated in absolute ethanol and water for 3 min, successively, the mirror-like GCE was dried with a fluid of highly purified nitrogen; the GCE was then treated with cyclic scanning in the potential range of 0.5–1.8 V at 20 mV s^{-1} for four scans in 0.001 mol l^{-1} L-tyrosine (ACN, 0.1 mol l^{-1} $NaClO_4$). To remove any physisorbed, unreacted materials from the electrode surface, the electrode was rinsed with ethanol and water and was sonicated for 3 min in pH 6.8 PBS. Then, the Tyr/GCE was obtained.

The Tyr/GCE was then immersed in the solution containing 0.05 mol l^{-1} OPD and 1.0 mol l^{-1} $HClO_4$ and treated by cycling between −0.25 and 1.3 V at 50 mV s^{-1} for 40 cycles. After being rinsed with water, the electrode was cycled again as above in solution containing only 1.0 mol l^{-1} $HClO_4$ for three scans to further polymerize the OPD monomer absorbed on/inside the film. Then, the poly (*o*-phenylenediamine)/L-tyrosine composite film modified GCE (referred as POPD-Tyr/GCE) was obtained and stored in 0.1 mol l^{-1} PBS (pH 6.8) at 4 °C for use.

Results and discussion

Electrode preparation

Preparation of GCE Generally speaking, before modification, the GCE should be pretreated via electrochemical oxidation in strong acid medium, such as H_2SO_4 solution; this process can produce oxygen-containing functionalities on GCE surface and even inside the carbon substrate, such as, carbonyl, quinoid, carboxylate, and hydroxyl radical species, etc. [21], and it is known that these oxygen-containing functional groups have somewhat electrochemical catalytic effect to the redox of some electro-active substances [21, 22]. In our study, we aimed to investigate the electrochemical activity and electro-catalysis of POPD doped by carboxylic groups in L-tyrosine; thus, it is necessary to avoid the influence of these oxygen-containing functional groups on GCE surface. Therefore, the GCE used should not be activated by potential scan (or polarized with positive potential) in strong acid medium, and it is also noted that, to avoid the exposing of GCE in air and thus the possible oxidation of carbon after the polishing and washing, the GCE should immediately be dried with a fluid of highly purified nitrogen and immersed in solution of L-tyrosine for grafting.

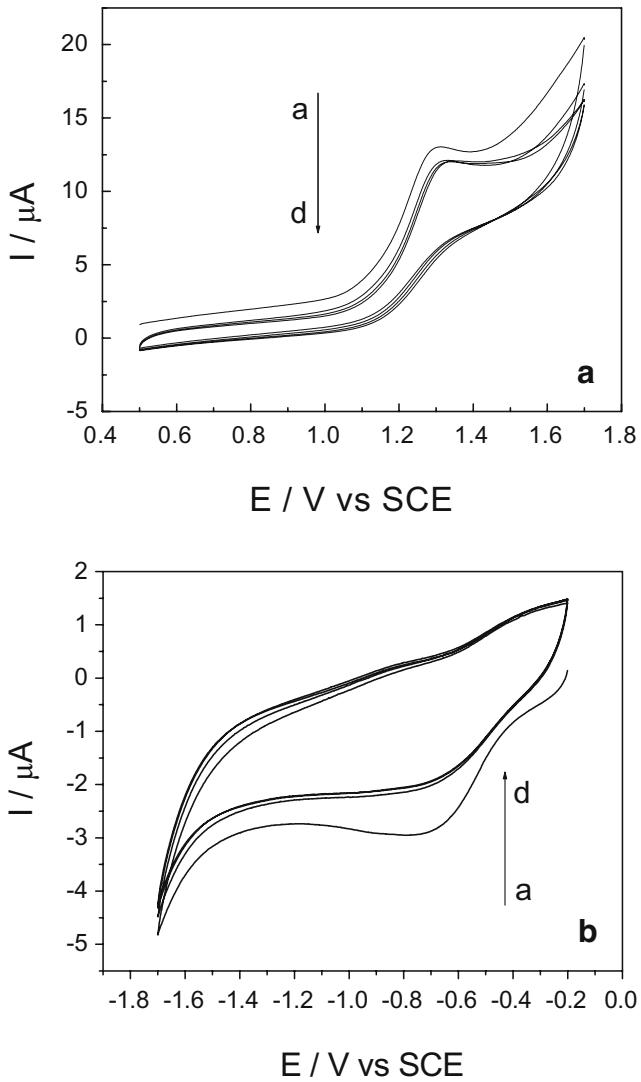

Fig. 1 **a** Cyclic voltammograms (*CVs*) of 0.001 mol l^{-1} L-tyrosine at GCE in ACN containing 0.1 mol l^{-1} $NaClO_4$; **b** CVs of Tyr/GCE in ACN solution containing 0.1 M $NaClO_4$. Scan rates: 0.05 V s^{-1}

Covalently grafting of L-tyrosine on GCE surface Figure 1a shows the cyclic voltammograms (CVs) of GCE in ACN solution containing 0.001 mol l^{-1} L-tyrosine and 0.1 mol l^{-1} $NaClO_4$ as supporting electrolyte. It can be seen from Fig. 1a that there is a broad, irreversible anodic peak at 1.30 V in the first cycle, and no cathodic peak is observed on the reverse scan, indicating that the species obtained after the first electron transfer undergoes a chemical reaction. One-electron oxidation of the amino group turns into its corresponding cation radical, and then, these cation radicals form C–N covalent bonds at the carbon electrode surface [23–25]. On the second cycle, the oxidation peak potential moves positively to 1.33 V, and the corresponding current response decreases quickly. In the following potential cycles, the anodic peak potential keeps stable, while the current response decreases somewhat until the fourth scan. The change of the current is attributed to the passivation of the carbon electrode; the passivation is related to the grafting of L-tyrosine onto the surface of GCE. The modification is almost complete after four cycles. As a primary amine, the electrochemical behavior of L-tyrosine is in accordance with the literature [24]. Thus, the EC modification process can be proposed as Scheme 1.

XPS analysis was employed to confirm the attachment of amine cation radicals on GCE surface. The position of N (1s) peak maximum at 398.6 eV, which is consistent with the formation of carbon–nitrogen bond between the amine cation radical and an aromatic moiety of GCE surface [23, 24], verify the immobilization of L-tyrosine on GCE surface (Fig. 2).

The surface density of amines on GCE was also studied. Once the molecule was bonded, it should be possible to observe its reduction. From the area of the reduction peak of the voltammogram, the number of molecules that were bonded can be deduced. After this, the L-tyrosine modified GCE was carefully ultrasonicated and transferred to ACN solution containing only 0.1 mol l^{-1} $NaClO_4$ for potential scan. The reduction voltammogram of Fig. 1b was then observed. As can be seen, the Tyr/GCE presents a well-defined reduction wave locating at about -0.80 V, corresponding to the reduction of the amine groups immobilized on GCE surface. The drawn-out voltammograms with successive scans may be due to the protonation of the radical anion by residual water. Knowing the surface area of the electrode, a concentration of 2.4×10^{-10} mol cm^{-2} can be calculated, indicating a monolayer surface coverage [26].

Electrochemical polymerization of OPD at Tyr/GCE Figure 3 shows the CVs for the electrochemical polymerization of OPD at Tyr/GCE in solution containing 0.05 mol l^{-1} OPD and 1.0 mol l^{-1} $HClO_4$ in the potential range of −0.25 and 1.30 V at 50 mV s^{-1}. In the first cycle, one broad oxidation peak with large anodic current appears at 0.69 V, indicating the formation of OPD radical cation through one-electron oxidation of the amino group. After the first cycle, however, this oxidation peak disappears, and a new oxidation peak appears at the potential of 0.60 V with a very lower oxidation current. On the reverse scan for the first circle, there is no corresponding cathodic appearance at the higher potential, indicating that the cation radicals are active and they attend to the reaction immediately. At the lower potential, two cathodic peaks present at 0.01 and −0.17 V, and then these two reduction peaks merge into one cathodic wave at −0.11 V with continuous cycling. In the following CVs, a broad anodic peak appears at −0.09 V. The pair of redox peaks at −0.09/−0.11 V is due to the redox of the POAP [27], and the currents increase slowly with an increase in the following potential scans.

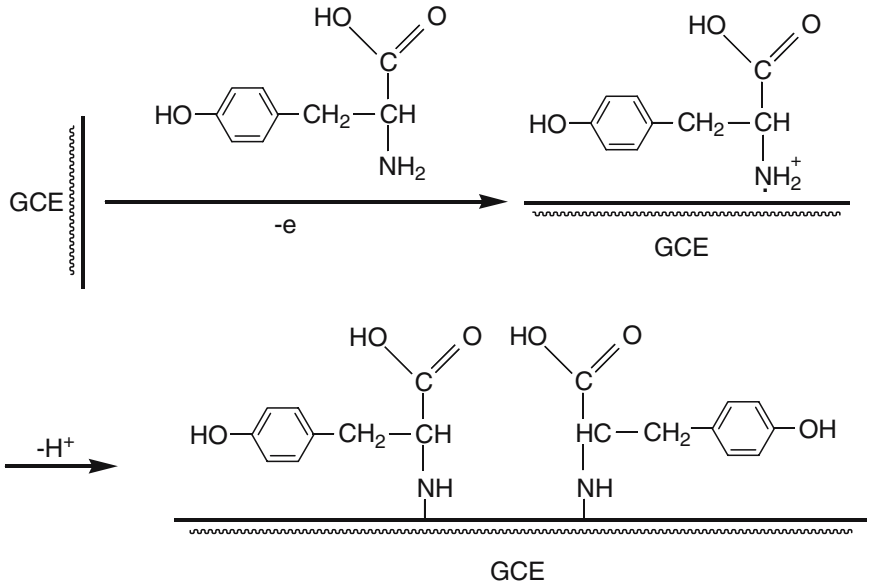

Scheme 1 EC modification process

Morphology of the polymer film The film prepared by the above procedure appears to be brown and non-uniform by visual inspection. SEM was employed to investigate the morphology of the POPD film on the L-tyrosine functionalized GCE. Figure 4 shows the micrograph of the POPD film polymerized after cyclically potential-scan for 40 cycles between −0.25 and 1.3 V at 50 mV s^{-1}. As can be seen, non-uniform POPD rings, bamboo-like fibrils (inset, right), and three dimensional net-works (inset, left) structures are obtained. The detailed mechanisms for the formation of these structures are not clear now. However, it can be assumed that the OPD monomers were firstly oxidized to their cation radicals; these cation radicals can act as "nuclear site" to direct the "linear growth/polymerization" of other OPD monomers in the same direction, and thus the bamboo-like fibrils were formed (inset, right). These bamboo-like fibrils with diameter of 50–120 nm and height of more than 400 nm stand upright on electrode surface. Whereas with the continuous increasing of the bamboo-like fibrils in length, the adjacent POPD fibrils standing upright on electrode surface grow to some "maximal length" and then tend/happen to contact together to form the stable ring-like and star-like structure. The star-like wires tend to connect together by dendrites to form 2D and further 3D net-works (inset, left). The bundles of POPD fibrils are organized in a non-periodic network of an average distance between contact points more than 500 nm. As to the formation of the ring-like shape with different size among the bamboo-like fibrils, two mechanisms can be assumed: one is that the adjacent POPD fibrils standing upright on the electrode

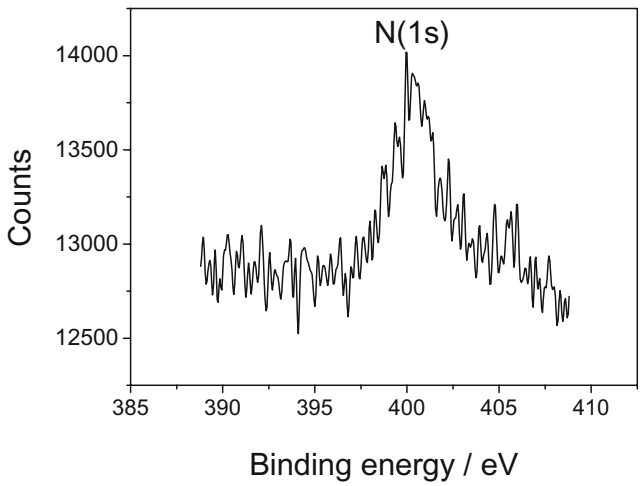

Fig. 2 XPS spectra for the Tyr/GCE showing the N(1s) peak

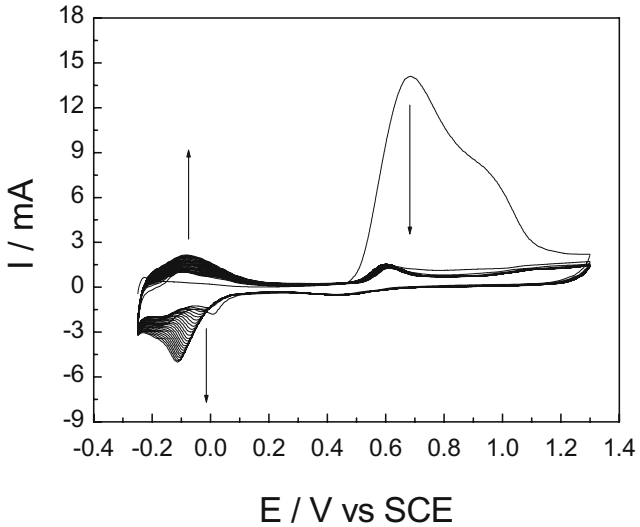

Fig. 3 CVs of 0.05 mol l^{-1} OPD at Tyr/GCE in 1.0 mol l^{-1} $HClO_4$ (υ=0.05 V s^{-1})

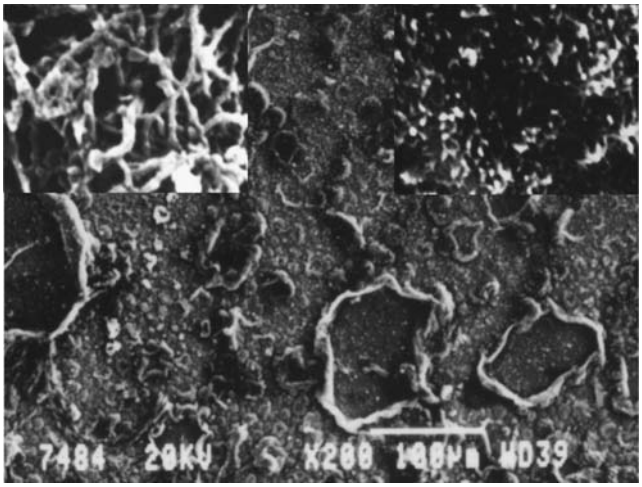

Fig. 4 SEM image of POPD formed by potential scanning of Tyr/GCE in 0.05 mol l^{-1} OPD and 1.0 mol l^{-1} $HClO_4$ between −0.25 and 1.3 V at 0.05 V s^{-1} for 40 cycles. The *inset* (*right*) shows the magnified bamboo-like POPD fibrils standing-up on electrode surface; and the *inset* (*left*) shows the magnified 3D net-works of POPD

surface grow to some "maximal length" and tend to contact together to form the POPD ring, a stable structure; the other, the postulation of "soup bubble" growth mechanism [28], may be ascribed to the formation of POA rings.

Redox electroactivity of POPD-Tyr/GCE

Figure 5 shows the CVs of POPD-Tyr/GCE (dotted lines) in various pH value solutions, and as a comparison, the CVs of POPD/GCE (solid lines) at different pH values are also given in Fig. 5. It can be seen that POPD/GCE shows good redox activity in strong acidic solution (solid lines of a and b). When the medium pH value increases to 5 (solid line of c), the reversibility of redox peaks becomes poor, and the response currents decrease obviously. With the continuous increasing of medium pH to 7, the reduction peak nearly disappears, and a broad oxidation wave with smaller current response can be seen (solid line of d). These results indicate that the electrochemical activity of POPD decreases gradually with increase of medium pH, and there is nearly no redox activity when medium pH increases up to 7. The redox peak currents decrease with increase of pH, which is attributed to the decrease in the apparent rate of charge transport in the POPD film. As for the composite film of POPD-Tyr, the POPD-Tyr/GCE shows good redox characteristics when medium pH increases up to pH 4 (omitted here). This indicates that the POPD-Tyr also has good electrochemical activity in acidic solution. When medium pH value increases to 5 (dotted line of e), POPD-Tyr/GCE presents a good pair of redox peaks, and the current is higher than that of POPD/GCE at the same pH value. When the pH value continually increases to 7 (dotted line of f), the POPD-Tyr/GCE still shows a good pair of redox peaks, indicating that the composite film can maintain its electrochemical activity even in neutral solution, which is favorable to its applications in bioelectrochemistry. These results show that the composite film of POPD-Tyr is electrochemically active in a fairly broad pH range. The improvement of electrochemical activity is caused by the doping of ionogenic –COOH groups of L-tyrosine, which insert in the POPD structure and change the local pH near the nitrogen atoms in the polymer, thus changing the micro-environment pH value [29, 30]. Therefore, a local acid–base balance is formed in the polymer, which is very stable and does not change in a broad pH range.

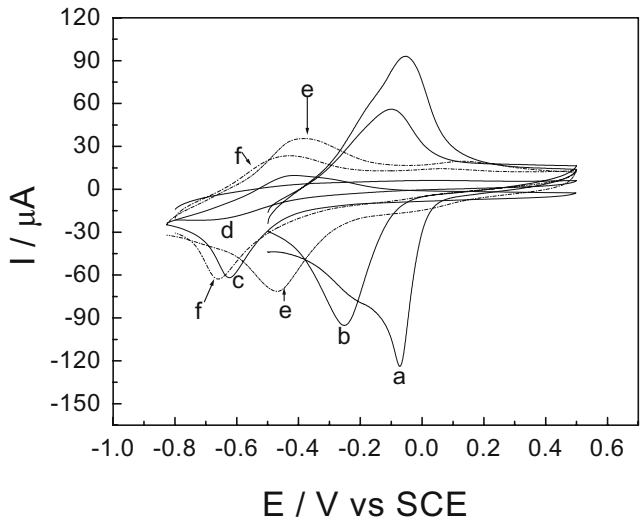

Fig. 5 CVs of POPD-Tyr/GCE (*dotted lines*) and POPD/GCE (*solid lines*) at different pH buffer solutions (*curve a* pH=1; *curve b* pH=3; *curves c and e* pH=5; *curves d and f* pH=7; υ=0.05 V s^{-1})

Electrochemical oxidation of AA at POPD-Tyr/GCE

Figure 6 shows the cyclic voltammograms of 5×10^{-4} mol l^{-1} AA at GCE (curve a), POPD-Tyr/GCE (curve b), and Tyr/GCE (curve c), respectively. It can be seen from Fig. 6 that the oxidation peak of AA is broad, irreproducible at 0.58 V with $E_p - E_{p/2} = 0.19$ V at GCE (curve a), and the oxidation current is about 11.2 μA. In contrast, the oxidation current (25 μA) increases greatly, and the peak potential shifts negatively to 0.35 V with $E_p - E_{p/2} = 0.08$ V at POPD-Tyr/GCE (curve b). The obviously increased peak current and the decrease in the anodic overpotential of about 0.23 V for AA indicate the strong electrocatalytic function of POPD-Tyr/GCE to the oxidation of AA. The shift in the overpotential is due to a kinetics effect; thus a substantial increase in the rate of electron transfer from AA is observed, which indicates the improvement in the reversibility of the electron transfer processes. As a comparison, the electrochemical behavior of AA at Tyr/GCE has also been

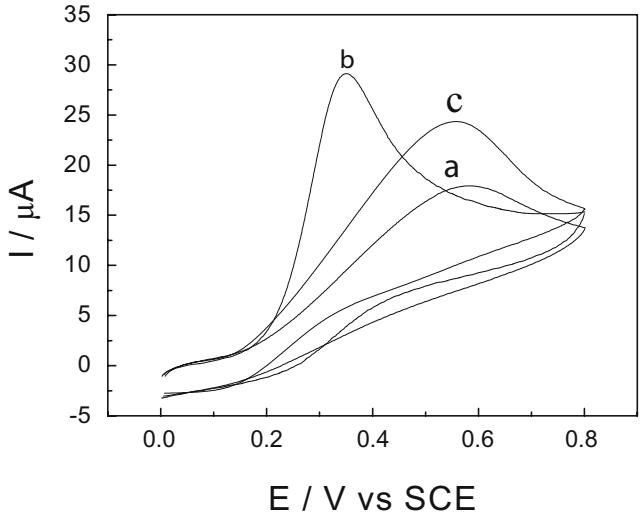

Fig. 6 CVs of 5×10^{-4} mol l^{-1} AA at GCE (*curve a*), POPD-Tyr/GCE (*curve b*), and Tyr/GCE (*curve c*) in 0.1 mol l^{-1}PBS (pH 6.8; υ=0.05 V s^{-1})

investigated (curve c); it can be seen from curve c that the oxidation potential of AA has a slightly negative shift (0.56 V) and somewhat increased peak current (17.5 μA) compared with that at GCE. This indicates that the obviously electrocatalytic oxidation of AA is mainly due to the POPD doped by L-tyrosine with carboxylic functionalities.

Figure 7 shows the CVs of POPD-Tyr/GCE at different concentrations of AA. As can be seen, the oxidation peak current increases linearly with increasing of AA concentration in the solution. The inset of Fig. 7 shows that the anode peak current is linearly dependent on the AA concentration in the range of 2.5×10^{-4}–1.5×10^{-3} mol l^{-1}, and the equation of linear regression is $i_p = (\mu A) = 0.2 + 0.4948c$ with a correlation coefficient of 0.9998.

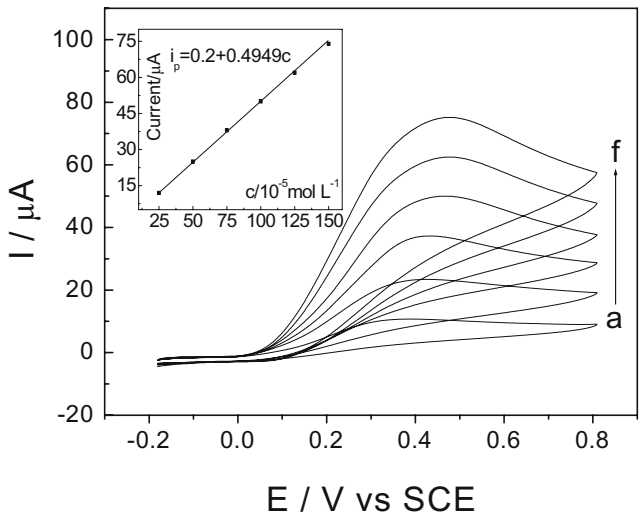

Fig. 7 CVs of different concentrations of AA at POPD-Tyr/GCE in 0.1 mol l^{-1} PBS (pH 6.8). Concentrations of AA from *curve a* to *f* are 2.5×10^{-4}, 5×10^{-4}, 7.5×10^{-4}, 1.0×10^{-3}, 1.25×10^{-3}, 1.5×10^{-3} mol l^{-1}, respectively (υ=50 mV s^{-1})

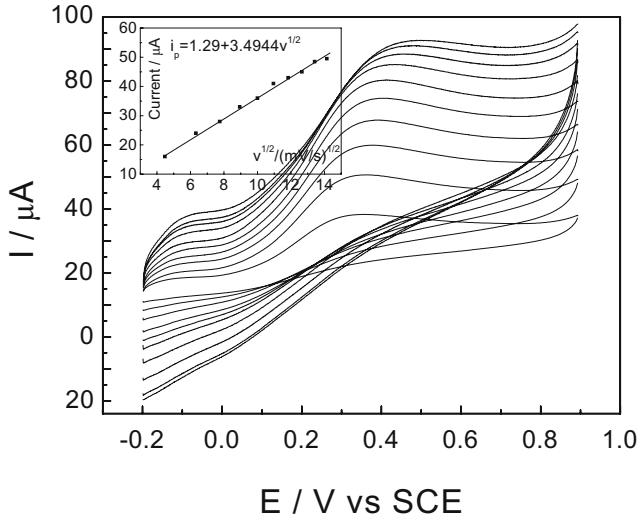

Fig. 8 CVs of 5×10^{-4} mol l^{-1} AA at POPD-Tyr/GCE in 0.1 mol l^{-1} PBS (pH 6.8) at different scan rates. Scan rates from down to up are 20, 40, 60, 80, 100, 120, 140, 160, 180, and 200 mV s^{-1}, respectively. *Inset* shows the calibration plot of i vs $\upsilon^{1/2}$

Further investigation was made into the transport characteristics of AA in the modified electrode. Figure 8 shows the CVs of POPD-Tyr/GCE in 5×10^{-4} mol l^{-1} AA solution at different scan rates. It can be seen that catalytic oxidation peak potential shifts to more positive with increasing scan rates, indicating a kinetics limitation in the reaction between the redox sites of POPD-Tyr film and AA. However, the cyclic voltammetric peak currents for AA oxidation at POPD-Tyr/GCE are proportional to the square root of scan rates in the range of 20–200 mV s^{-1} (inset of Fig. 8) indicating that the electrode reaction is controlled by diffusion-controlled process. The equation of linear regression is $i_p(\mathrm{uA}) = 1.29 + 3.4944\nu^{1/2}$ with a correlation coefficient of 0.9975.

Analytical characterization

To investigate the real practice of the POPD-Tyr/GCE, the amount of AA in vitamin C tablet has been detected using the suggested procedure. A tablet of vitamin C (10 mg per tablet) was first dissolved in 40 ml 0.1 mol l^{-1} PBS

Table 1 Determination and recoveries of AA in vitamin C tablet

Sample no.	AA content (μg)	AA detected[a] (μg)	Spike (μg)	After spike[a] (μg)	Recovery[a] (%)
1	300	292.6	88.1	364.2	93.8
2	300	286.7	132.2	400.3	92.6
3	300	288.2	176.2	446.8	93.8
4	300	290.4	220.3	492.3	94.7
Average		289.5			93.7

[a] The mean value of five determination results

(pH 6.8), after which filtration the AA solution was transferred into 100 ml volumetric flask and diluted to volume with 0.1 mol l^{-1} PBS (pH 6.8); thus, an AA solution with content of 5.68×10^{-4} mol l^{-1} (100 μg ml^{-1}) was obtained. Then, 3.0 ml of the sample solution was placed into a home-made electrochemical cell, and the concentration of AA was determined by the calibration method. The results are listed in Table 1. To ascertain the validity of the proposed procedure based on the POPD-Tyr/GCE, the samples were spiked with certain amounts of standard AA solution (0.05 mol l^{-1}), and then, the total amount of AA was measured (see Table 1). The recovery rates of the spiked samples were estimated to be between 92.6 and 94.7%.

Electrode stability, reproducibility, and detection limit

Because the procedure of electrode preparation was easy and rapid, it was not important for the electrode to be stable for a prolonged time. However, the long-term stability of the modified electrode has also been checked by measuring the response from day to day during a storage in 0.1 mol l^{-1} PBS (pH 6.8) at 4 °C. During the first 2 days, the current response had no apparent change, and in the next 7 days, the current response decreased about 12% of its initial response and 17% for 1 month.

To characterize the reproducibility of the POPD-Tyr/GCE, repetitive measurements were carried out in solutions containing 5×10^{-4} mol l^{-1} AA. The results of ten successive measurements showed a relative standard deviation of 3.2% for AA, indicating that the modified electrode was not subject to surface fouling by the oxidation products.

To evaluate the detection limit of the proposed analytical procedure, the responses of 11 reagent blank samples have been measured; the relatively standard derivation (δ) was calculated to be 7.2×10^{-3}. Based on the slope (s) of the working curve of 1.67 μA mM^{-1}, the detection limit ($3\delta/s$) can be estimated to be 12.93 μM.

Conclusions

This study reported the electrochemical polymerization of *o*-phenylenediamine on L-tyrosine functionalized GCE, and due to the doping of POPD by carboxylic functionalities in L-tyrosine, the electrochemical activity of POPD was extended to neutral medium. At pH 6.8 PBS, the POPD-Tyr/GCE electrode shows good electrocatalytic activity towards the oxidation of AA via a surface layer-mediated charge transfer. Because the L-tyrosine layer was covalently grafted on GCE surface, the composite film of POPD-Tyr was very stable, and the proposed procedure can be used for the determination of AA in real sample.

Acknowledgements The authors wish to acknowledge the financial support of this paper by Shanghai Leading Academic Discipline Project (T0402), Shanghai Municipal Education Commission (05DZ16), and Shanghai Normal University (PL507).

References

1. Martin DW Jr (1983) In: Martin DW Jr, Mayes PA, Rodwell VW (eds) Harper's review of biochemistry. 19st edn. Lange, LosAltos, CA, p 112
2. Koshiishi I, Imanari T (1997) Anal Chem 69:216–220
3. Ueda C, Chi-Sing Tse D, Kuwana T (1982) Anal Chem 54:850–856
4. Murthy ASN, Anita (1994) Biosens Bioelectron 9:439–444
5. Pournaghi-Azar MH, Razmi-Nerbin H (2000) J Electroanal Chem 488:17–24
6. Zhang L, Sun Y, Lin X (2001) Analyst 126:1760–1763
7. Zhang L, Lin X (2001) Analyst 126:367–370
8. Zhang L, Jia JB, Zou XQ, Dong SJ (2004) Electroanalysis 16:1413–1418
9. Mao H, Pickup PG (1989) J Electroanal Chem 265:127–142
10. Lyons MEG, Breen W, Cassidy J (1991) J Chem Soc, Faraday Trans 87:115–123
11. Zhou D, Xu J, Chen H, Fang H (1997) Electroanalysis 9:1185–1188
12. Xu JJ, Zhou DM, Chen HY (1998) Fresenius J Anal Chem 362:234–238
13. Zhang L (2007) J Solid State Electrochem 11:365–371
14. Cai LT, Chen HY (1999) Sensors and Actuators B 55:14–18
15. Golabi SM, Nozad A (2002) J Electroanal Chem 521:161–167
16. Malitesta C, Losito I, Zambonin PG (1999) Anal Chem 71:1366–1370
17. Karalemas ID, Georgiou CA, Papastathopoulos DS (2000) Talanta 53:391–402
18. Tonosaki T, Oho T, Isomura K, Ogura K (2002) J Electroanal Chem 520:89–93
19. Yano J, Terayama K, Yamasaki S (1996) J Mater Sci 31:4785–4792
20. Yano J, Yamasaki S (1999) Synth Met 102:1157
21. Cai XH, Kalcher K, Neuhold C, Ogorevc B (1994) Talanta 41:407–413
22. Nagaoka T, Yoshino T (1986) Anal Chem 58:1037–1042
23. Barbier B, Pinson J, Desarmot G, Sanchez M (1990) J Electrochem Soc 137:1757–1764
24. Deinhammar RS, Ho M, Anderegg JW, Porter MD (1994) Langmuir 10:1306–1313
25. Downard AJ, Mohamed A (1999) Electroanalysis 11:418–423
26. Cheng Q, Brajter-Toth A (1996) Anal Chem 68:4180–4185
27. Sivakkumar SR, Saraswathi R (2004) J Appl Electrochem 34:1147–1152
28. Qu L, Shi G, Chen F, Zhang J (2003) Macromolecules 36:1063–1067
29. Karyakin AA, Strakhova AK, Yatsimirsky AK (1994) J Electroanal Chem 371:259–265
30. Sun JJ, Zhou DM, Fang HQ, Chen HY (1998) Talanta 45:851–856